Open Journal of Civil Engineering, 2020, 10, 195-212
https://www.scirp.org/journal/ojce
ISSN Online: 2164-3172
ISSN Print: 2164-3164

Evaluation of Dynamic Modulus of HMA Sigmoidal Prediction Models and Optimization by Approach of U.S. Mesh Sieve by AFNOR and LC Mesh Sieve

Mouhamed Lamine Chérif Aidara[1], Makhaly Ba[1], Alan Carter[2]

[1]UFR Sciences de l'Ingénieur, Université de Thiès, Thiès, Sénégal
[2]Ecole de Technologie Supérieure (ETS), Director of Pavement BituminousMaterials Laboratory (LCMB), Montréal, Canada
Email: mouhamedlamine.aidara@univ-thies.sn

How to cite this paper: Aidara, M.L.C., Ba, M. and Carter, A. (2020) Evaluation of Dynamic Modulus of HMA Sigmoidal Prediction Models and Optimization by Approach of U.S. Mesh Sieve by AFNOR and LC Mesh Sieve. *Open Journal of Civil Engineering*, **10**, 195-212.
https://doi.org/10.4236/ojce.2020.103017

Received: July 3, 2020
Accepted: July 21, 2020
Published: July 24, 2020

Abstract

Pavement design tools are not universal. Indeed, in the sizing of pavements in the USA, the prediction models used in the calculation of the dynamic modulus of HMA are not adapted to the characterization of the mineral skeleton of the HMA mix designed with the French method. This article aims to assess the predictive models of the dynamic modulus used in the mechanistic-empirical design for their use in the design of bituminous pavements, and to develop new predictive models taking into account the sieve series LC and AFNOR standards. A total of six types of mixtures were subjected to the determination of complex modulus testing by direct tensile-compression on cylindrical specimens (26-700 LC) over a temperature range (5) and frequency (5) data. Dynamic modulus prediction models $|E^*|$ are studied Witczak model 1999 and model Witczak 2006. These models do not take into account the AFNOR or LC mesh sieve, an approach was made in relation to the US mesh sieve to replace ρ_{200} (0.075 mm), ρ_4 (4.76 mm), ρ_{38} (9.5 mm) and ρ_{34} (19 mm) respectively by the AFNOR mesh $P_{0.08}$ (0.08 mm), R_5 (5 mm), R_{10} (10 mm) and R_{14} (14 mm). The result is the production of two models whose are evaluated by correlation with the values $|E^*|$ of modulus measured in the laboratory is satisfactory (R^2 = 0.83 respectively R^2 = 0.71 and p-value = 0.00). The optimization of these approximate models gave new models with the same frame as the original models and a better correlation with the data observed in the laboratory (respectively R^2 = 0. 95 and R^2 = 0.91 p-value = 0.00).

Keywords

Dynamic Modulus, Mechanistic-Empirical Design, US, Sieve, Mesh, HMA, AFNOR, LC

1. Introduction

In Mechanistical Empirical Design [1] (Hammons, 2007) the bituminous layer at level 2 and 3 requires the use of prediction model because at level 1 (highest reliability level) the dynamic modulus of Hot Mixture Asphalt (HMA) coatings is determined by laboratory tests [2] [3] [4] [5]. However, when these HMA are mix designed according to the French method with aggregates specified with different sieve mesh, the use of American models is no longer possible. This justifies the need to find a solution. One of the main parameters characterizing the behavior of "Hot Mixture Asphalt" (HMA) in the "Mechanistic-Empirical Pavement Design Guide" (M-EPDG) is the dynamic modulus. However, it has three levels of characterization in this design method. Level 1 is the most accurate, and requires the determination by laboratory tests of the dynamic modulus and Poisson's ratio of each type of mix involved in the pavement structure. The second and third level require the use of a master curve model from a prediction equation developed by the "National Cooperative Highway Research Program" (NCHRP) team [6]. In the dynamic modulus prediction approach for HMA, they exist two main methods. The first is called a discrete finite element method [7] [8] [9]; and a second method using empirical equations [9] [10] or micro prediction equations [9] [11]. The two best-known empirical models are the 1999 Witczak's model and the 2006 Witczak's model. They are characterized by the same parameters except that the viscosity of the binder and the loading frequency directly considered in the 1999 model are replaced by the shear modulus ($|G^*|$) and the phase angle of the binder (δ_b). Parameters related to the granularity of the bituminous mixture in Witczak's empirical models are specified according to US mesh screen (US Standard Series) described by the "American Association of highway and Transportation Official" (AASHTO) standards named 37.5 mm, 25.0 mm, 19.0 mm, 12.5 mm, 9.5 mm, 4.75 mm, 2.36 mm, 1.18 mm, 0.60 mm, 0.30 mm, 0.15 mm and 0.075 mm. What makes these models almost impossible to use when the sieve mesh from "Canadian Standard Series" (LC) or from French Standards Association (AFNOR) standards are used to learn about the two 14 mm, 10 mm, 8 mm, 5 mm, 2.5 mm, 1.25 mm, 0.315 mm, 0.16 mm and 0.08 mm. However, a statistical approach remains possible, because Witczak's models are statistical models of sigmoidal type. These models are determined from only database from laboratory tests [4]. In order to make this approach possible similar tests have been carried out.

In this study, the dynamic modulus of asphalt mixtures with aggregate skeletons specified according to AFNOR and Lc sieve are determined by US sieve mesh approach by using the 1999 and 2006 Witczak's models. The aggregates of Senegal used are basalt from Diack and quartzite from Bakel. Bitumen is 35/50 (AFNOR) grade (or pavement grade PG 70/16) ERES.

This article will statistically measure the impact of the approach on the prediction of the dynamic modulus and develop an empirical model whose parameters related to the particle size of the mixture were specified according to Standard French Normalization Association (AFNOR) and Québec Publication (LC) mesh sieve.

2. Methodology

The objectives of this paper are to assess the Witczak sigmoidal model prediction of the dynamic modulus for HMA by approaching sieve mesh considered and to develop a new predictive model based on the AFNOR standards sieve mesh and LC by a non-linear optimization in Solver-Microsoft Excel.

A total of six mixtures designed according to the Marshall method and validated according to the level 4 of HMA mix design procedures [12] is studied. Two aggregates types and two nominal maximum aggregate size (NMAS) are used in the different formulation with a single type of bitumen (grade 35/50 ERES or PG70/16). The specimens were cored from asphalt plate compacted to LCPC compactor. They have a height of 125 mm and a diameter of 74 mm with a void percentage interval ranging from 2% to 8%. Direct tension-compression test on cylindrical specimens is used for the measurement of the dynamic modulus mixtures studied. The results of the test on the DSR ERES 35/50 bitumen are used for determining the parameters models related to the asphalt binder (A, VTS, η, δ_b and G^*).

2.1. The Test Dynamic Shear Rheometer

DSR is a test for measuring the rheological stiffness and elasticity binders and bituminous mastics through the dynamic shear modulus G* and the δ phase angle [13]. It applies to high temperatures and intermediaries usually an old bitumen from "Rolling Thin Film Oven Test" (RTFOT). To input data requirements for writing prediction models studied, the DSR tests were performed at the same temperature (55˚C, 40˚C, 30˚C, 20˚C and 10˚C) and frequencies (10 Hz, 5 Hz, 1 Hz, 0.3 Hz and 0.1 Hz) than the dynamic modulus is testing.

2.2. Direct Tension-Compression Test on Cylindrical Specimen

The complex modulus tests are performed according to standard [13] entitled "Determination of the complex modulus of HMA" by using direct tension-compression equipment (TCD) on cylindrical specimens (**Figure 1**). E^* is determined at small strains, at different frequencies and temperatures, in order to characterize the linear viscoelastic behavior of the mix. E^* is a complex number which consists of two parameters, namely the dynamic modulus ($|E^*|$), which is the standard of E^*, and the phase angle (δ), which is the argument of E^*. The $|E^*|$ is used for pavement design and δ can appreciate the viscoelastic behavior of the asphalt.

Figure 2 illustrates the results of a complex modulus test with the offset observed between the stress measurement and those deformations [9].

The complex modulus E^* is determined by Equation (1).

http://www.bitumequebec.ca/wp-content/uploads/2015/03/594ccf2a184885dfile.pdf

Figure 1. HMA specimen on the direct tension-compression equipment [14].

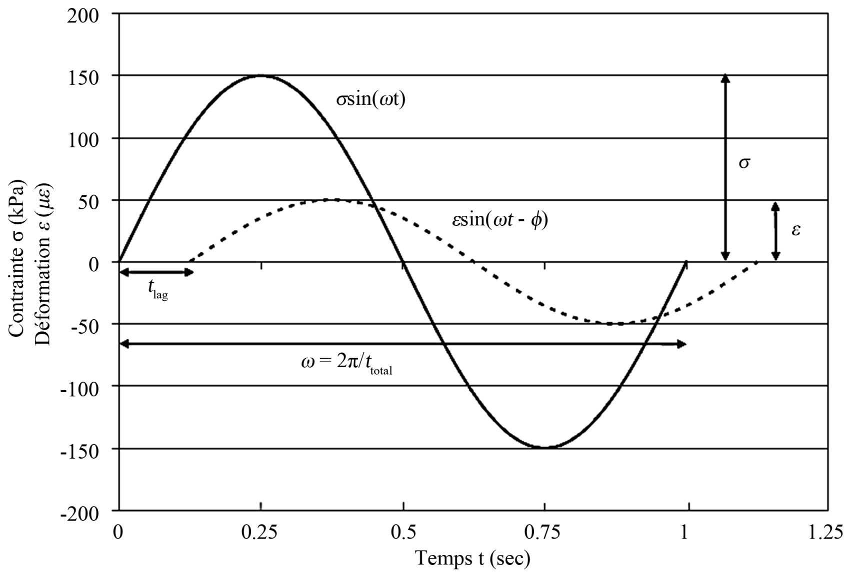

Figure 2. Sinusoidal stress and deformation in tension-compression test [14].

$$E^{*} = \frac{\sigma \sin(\omega t + \varphi)}{\varepsilon \sin(\omega t - \varphi)} = |E^{*}| \cos\varphi + i |E^{*}| \sin\varphi \tag{1}$$

[14].

Dynamic modulus $|E^*|$ is given by Equation (2) [4]

$$|E^{*}| = \frac{\sigma}{\varepsilon} = \frac{4P/\pi d^{2}}{\delta h/h} \tag{2}$$

[14].

The phase angle is determined by Equation (3).

$$\varphi = \omega t_{l\partial g} \tag{3}$$

(Touhara)

where E^* is the complex modulus (kPa); $|E^*|$ is the dynamic modulus (kPa); φ is the phase angle (rad); σ is the total axial stress (kPa); ε is the total axial deformation (m/m); ω is the period (2·π·*f*) (rad); *t* is time (sec); "*I*" is the imaginary number; t_{lag} is time to shift between s and e (sec); *P* is the axial load (kN); *d* is the diameter of the test piece (m);. Δh is the axial displacement (m); and *h*: height for measuring. Δh (100 mm) (m).

2.3. The Model 1999 Witczak's Model

The 1999 Witczak's model is used in levels 2 and 3 of pavement design. It is given by Equation (4).

$$\begin{aligned}\log\left|E^*\right| = & -1.249937 + 0.029232\rho_{200} - 0.001767\left(\rho_{200}\right)^2 - 0.002841\rho_4 \\ & - 0.058097V_a - 0.0802208\left(\frac{V_{beff}}{V_{beff}+V_a}\right) \\ & + \frac{3.871977 - 0.0021\rho_4 + 0.003958\rho_{38} - 0.000017\left(\rho_{38}\right)^2 + 0.005470\rho_{34}}{1+\mathrm{e}^{\left(-0.603313-0.31335\log(f)-0.395321\log(\eta)\right)}}\end{aligned} \quad (4)$$

[4].

With $|E^*|$ is the dynamic modulus (105 psi); η is the viscosity of the binder (106 poise); *f* is the loading frequency in Hz; ρ_{200} is the percentage passing through a sieve 0.075 mm (No. 200); ρ_4 cumulative percentage of the sieve 4.76 mm (No. 4); ρ_{38} is the cumulative percentage of the sieve 9.5 mm (3/8 in); ρ_{34} is the cumulative percentage of the sieve, 19 mm (3/4 in); V_a is the air void percentage; V_{beff} is effective binder content in percentage volume.

In fact in the report of NCHRP 1-37A it was developed by recalibration of the dynamic modulus of the prediction model developed by Witczak and Fonseca [10]. It was made by adding a new database to the original database. The evaluation of the reliability of the original model on the original database gave R^2 = 0.87 precision and Se/Sy 0.36 in basic arithmetic and assessment of its reliability on the new database is less accurate with R^2 = 0.73 and Se/Sy = 0.53. These observed differences assigned to differences in granularity and bitumen in the mixtures of the two databases. The results of the recalibration on the reliability of the model Witczak 1999 was satisfactory with an R^2 of 0.941, and Se/Sy 0.2449 [4].

2.4. The Model Witczak 2006

However, the 1999 Witczak model poses a problem related to the fact the rigidity of the binder is characterized by a viscosity that does not take into account the effects of the charging frequency. In this model the frequency it is considered as another independent variable entered the predictive equation. However, the viscosity of the binder depends on the charging frequency. Thus changes in the load frequency induce changes of viscosity of the binder. From this point of view the scenario presented by the 1999 model where binder viscosity remains constant when the load frequency changes cannot be conceived in reality. In 2006 Bari and Witczak taking into account remarks cited above set of 7400 modulus measurements from 346 mixtures of HMA presents a new model in which the viscosity of the binder and the loading frequency considered directly in the model 1999 are replaced by the shear modulus $|G^*|$ and the phase angle. δ_b of the binder [11]. This model is described by Equation (5)

$$\log\left|E^*\right| = -0.349 + 0.754\left(\left|G_b^*\right|^{-0.0052}\right)\times\left(6.65 - 0.032\rho_{200} + \left(0.0027\rho_{200}\right)^2 + 0.011\rho_4 - 0.0001\left(\rho_4\right)^2 + 0.006\rho_{38} - 0.00014\left(\rho_{38}\right)^2 - 0.08V_a - 0.16\left(\frac{V_{beff}}{V_a + V_{beff}}\right)\right) + \frac{2.558 + 0.032V_a + 0.713\left(\frac{V_{beff}}{V_a + V_{beff}}\right) + 0.0124\rho_{38} - 0.0001\left(\rho_{38}\right)^2 - 0.0098\rho_{34}}{1 + e^{\left(-0.7814 - 0.5785\log\left|G_b^*\right| + 0.8834\log\delta_b\right)}} \quad (5)$$

[11].

where $|E^*|$ is the dynamic modulus (psi); $|G^*|$ is the dynamic shear modulus of the binder; δ_b is the binder phase angle; ρ_{200} = % of sieving 200; ρ_4 = % cumulative screen oversize 4; ρ_{38} = % cumulative screen oversize 3/8; ρ_{34} = % refusal cumulative ¾ screen; V_a = % air void; V_{beff} = effective binder content.

2.5. Statistical Interpretations

The 1999 and 2006 Witczak's models are nonlinear models (polynomial) as a sigmoidal function. Their development was based on the analysis and optimization of the statistical process.

Statistical analysis was intended to reduce the prediction error by comparing the predicted values with the measured values [5].

The nonlinear optimization is to find the values of the regression coefficients or adjustment parameters used in a model so that the model equation has a minimum error when a set of predicted and measured data are compared (Bari and Witczak, 2006).

The goodness of fit indicates the degree of binding of the adjustment parameters to the prediction model. The nonlinear optimization uses as indicator the determination coefficient R^2 and the ratio of the standard error (Se) and standard deviation (Sy) noted Se/Sy. A good model present a high R^2 (close to unity) and a low Se/Sy.

Statistical quality of the correlation is given by R^2 and usually taken p-value of $p < 0.005$. It is the latter that will be used in the interpretation of our results.

The complex structure of HMA explains the choice of nonlinear optimization to study the predictive models.

The Solver Microsoft Excel is a useful and precise function chosen by most researchers to optimize the nonlinear problems. When the sum of the squared error is minimized, the solution is a biased solution.

The database used to make the calculations are presented as an appendix at the end of the article.

2.6. Model Variables

The analysis of the data consists of 1999 and 2006 Witczak's model parameters *i.e.* $|G^*|$, f, η, δ_b, ρ_{200}, ρ_4, ρ_{38}, ρ_{34}, V_a and V_{beff}. They are the explanatory or independent variables to predict the dependent variable $\log|E^*|$ (explain). However, the values of the sieve meshes are approached $P_{0.08}$ (ρ_{200}), R_{10} (ρ_{38}), R_{14} (ρ_{34}) and R_5 (ρ_4).

NB: η values were determined from the coefficients ASTM A + VTS. This results in Equations (6) and (7) below.

$$\begin{aligned}\log\left|E^*\right| &= -1.249937 + 0.029232P_{0.08} - 0.001767\left(P_{0.08}\right)^2 \\ &- 0.002841R_5 - 0.058097V_a - 0.0802208\left(\frac{V_{beff}}{V_{beff}+V_a}\right) \\ &+ \frac{3.871977 - 0.0021R_5 + 0.003958R_{10} - 0.000017\left(R_{10}\right)^2 + 0.005470R_{14}}{1+e^{\left(-0.603313-0.31335\log(f)-0.395321\log(\eta)\right)}}\end{aligned} \tag{6}$$

With $|E^*|$ = dynamic modulus (105 psi); η = viscosity of the binder (106 poise); f = frequency in Hz loading; P_{200} = percent passing sieve 0.08 mm; R_5 = cumulative percentage of the sieve 5 mm; R_{10} = the percentage of cumulative screen oversize 10 mm; R_{14} = the percentage of cumulative screen oversize 14 mm; V_a = percentage of vacuum; V_{beff} = Binder content effective in percentage volume.

$$\begin{aligned}\log E^* &= -0.349 + 0.754\left(\left|G_b^*\right|^{-0.0052}\right)\times\Bigg(6.65 - 0.032P_{0.08} \\ &+ \left(0.0027P_{0.08}\right)^2 + 0.011R_5 - 0.0001\left(R_5\right)^2 + 0.006R_{10} \\ &- 0.00014\left(R_{10}\right)^2 - 0.08V_a - 0.16\left(\frac{V_{beff}}{V_a+V_{beff}}\right)\Bigg) \\ &+ \frac{2.558 + 0.032V_a + 0.713\left(\frac{V_{beff}}{V_a+V_{beff}}\right) + 0.0124R_{10} - 0.0001\left(R_{10}\right)^2 - 0.0098R_{14}}{1+e^{\left(-0.7814-0.5785\log\left|G_b^*\right|+0.8834\log\delta_b\right)}}\end{aligned} \tag{7}$$

With $|E^*|$ = dynamic modulus (105 psi); $|G^*|$ is the dynamic shear modulus of the binder; δ_b is the phase angle of the binder $P_{0.08}$ = percent passing 0.08 mm sieve; R_5 = cumulative percentage of the sieve 5 mm; R_{10} = the percentage of cumulative screen oversize 10 mm; R_{14} = the percentage of cumulative screen oversize 14 mm; V_a = void percentage; V_{beff} = Binder content effective in percentage volume.

3. Results

3.1. Evaluation 1999 Witczak's Approached Model

A correlation is performed on the values of modulus predicted by sieve mesh with the approximate 1999 Witczak's model and the values measured in the laboratory on the mixtures designed with the basalt Diack and the quartzite Bakel by direct tensile/compression tests test on cylindrical specimens.

Figure 3 shows a fairly good estimate of the 1999 Witczak's model with a very strong correlation of $R^2 = 0.83$ and a significant p ($p = 0.00$).

3.2. Adjustment and Optimization of 1999 Witczak's Approached Model

Table 1 shows the optimized coefficients Witczak module 1999 in comparison to the initial coefficients.

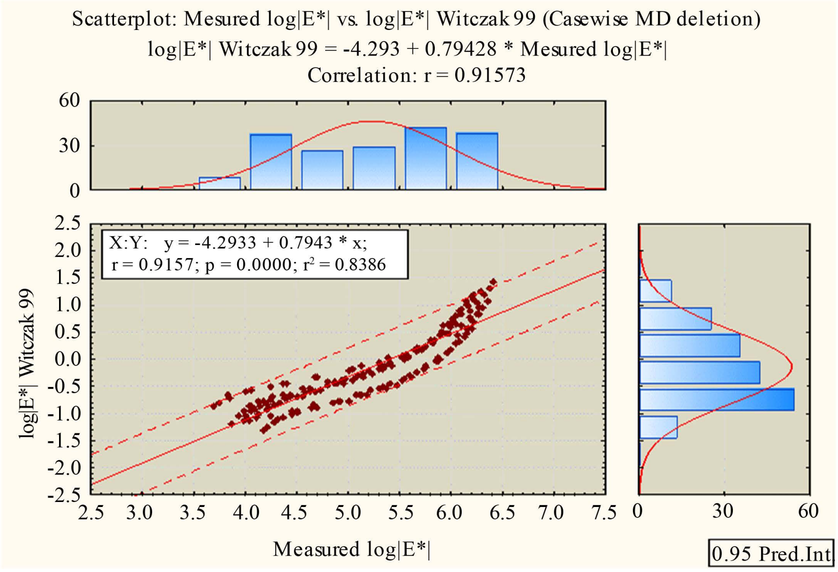

Figure 3. Correlation $p < 0.005$ for log|E^*| and predicted log|E^*| observed.

Table 1. Comparison of the optimized regression coefficients and the initial coefficients.

Régression coefficients	Optimized coefficients	Initial coefficients
F1	0.152593542	1.249937
F2	0.006186186	0.029232
F3	0.003011471	0.001767
F4	0.002858835	0.002841
F5	0.0000001	0.058097
F6	0.088945463	0.0802208
F7	7.698304773	3.871977
F8	0.00194078	0.0021
F9	0.003636243	0.003958
F10	1.72114E-05	0.000017
F11	0.003804769	0.00547
F12	1.90175288	0.603313
F13	0.205909497	0.31335
F14	0.284943589	0.395321
Sum of squared deviations	4.56	

The new 1999 Witczak's approached model and optimized is given by Equation (8) below:

$$\log\left|E^*\right| = -0.152593542 + 0.006186186P_{0.08} - 0.003011471\left(P_{0.08}\right)^2 - 0.002858835R_5 - 0.00000017V_a - 0.088945463\left(\frac{V_{beff}}{V_{beff}+V_a}\right) + \frac{7.698304773 - 0.00194078R_5 + 0.003636243R_{10} - 1.72114E-05\left(R_{10}\right)^2 + 0.003804769R_{14}}{1+e^{\left(-1.90175288-0.205909497\log(f)-0.2849435891\log(\eta)\right)}} \quad (8)$$

With $|E^*|$ = dynamic modulus (105 psi); η = viscosity of the binder (106 poise); f = frequency in Hz; P_{200} = percent passing sieve 0.08 mm; R_5 = cumulative percentage of the sieve 5 mm; R_{10} = the percentage of cumulative screen oversize 10 mm; R_{14} = the percentage of cumulative screen oversize 14 mm; V_a = void percentage; V_{beff} = Binder content effective in percentage volume.

Correlating the predicted modulus values with the new approached model values shows a good correlation with an R^2 = 0.9574 and p = 0.00. Figure 4 illustrate the results of the correlation.

3.3. Evaluation 2006 Witczak's Approached Model

A correlation is performed on the values of modulus predicted by sieve mesh with the approximate 2006 Witczak's model and the values measured in the laboratory show a fairly good estimate of the model Witczak 1999 with a very strong correlation of R^2 = 0.71 and a significant p (p = 0.00) (Figure 5). A non-linear optimization by the MS Excel Solver may however be used to improve the correlation.

3.4. Adjustment and Optimization of 2006 Witczak's Approached Model

Table 2 shows the optimized coefficients of 2006 Witczak's model in comparison to the initial coefficients. The optimization shows that the coefficient F11 is

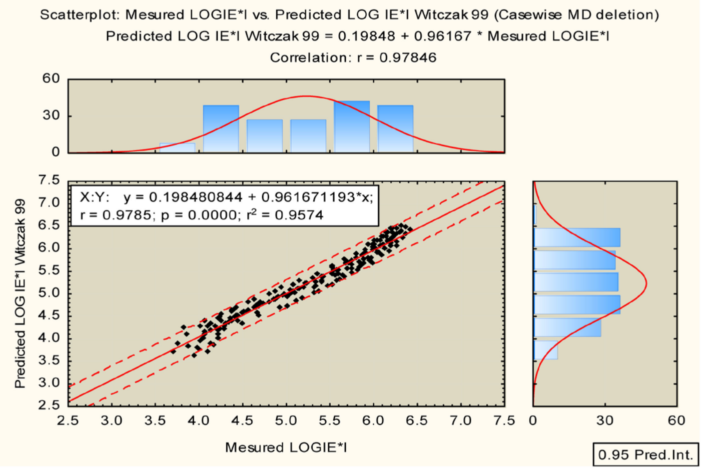

Figure 4. Correlation $p < 0.005$ $\log|E^*|$ predicted, optimized and $\log|E^*|$ observed.

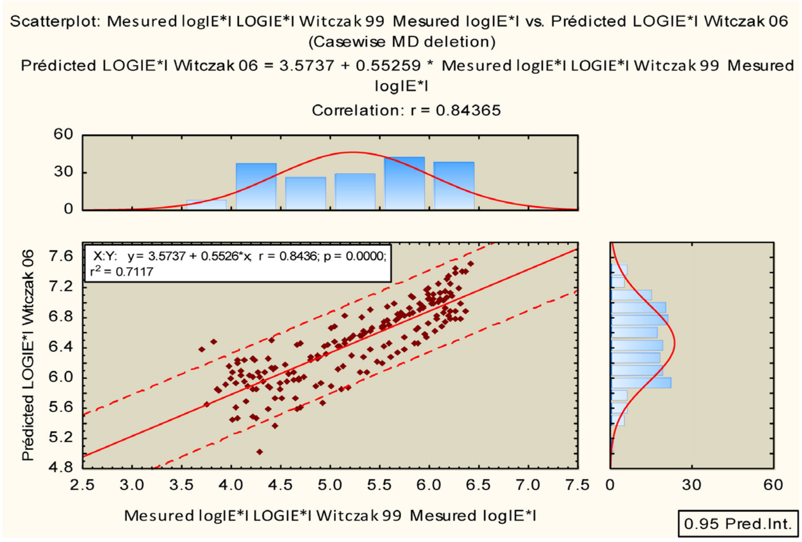

Figure 5. Correlation $p < 0.005$ for $\log|E^*|$ and predicted $\log|E^*|$ observed.

Table 2. The optimized regression coefficients and the initial coefficients.

Régression coefficients	Optimized coefficients	Initial coefficients
F1	0.354624896	0.349
F2	0.73016561	0.754
F3	0.005481779	0.0052
F4	5.461922604	6.65
F5	0.036114863	0.032
F6	0.002060831	0.0027
F7	0.005137335	0.011
F8	0.000128808	0.0001
F9	0.003963945	0.006
F10	0.000166591	0.00014
F11	0.0000001	0.08
F12	0.18414392	0.16
F13	2.597758994	2.558
F14	0.040197991	0.032
F15	0.596946197	0.713
F16	0.00806974	0.012
F17	0.000106102	0.0001
F18	0.010347472	0.0098
F19	0.847277886	0.7814
F20	0.80288457	0.5851
F21	1.540388406	0.8834
Sum of squared deviations	85.49290941	

canceled by the solver. However, in order to keep the shape intact models, a lower value of this coefficient is chosen so as not to vary the SSD significantly. The new model 2006 Witczak's approached model optimized is given by Equation (9) below.

$$\log E^* = -0,354624896 + 0.73016561\left(\left|G_b^*\right|^{-0.005481779}\right)$$
$$\times\Bigg(5.461922604 - 0.036114863P_{0.08} + \left(0.002060831P_{0.08}\right)^2 + 0.005137335R_5$$
$$-0.0.000128808\left(R_5\right)^2 + 0.0.003963945R_{10} - 0.000166591\left(R_{10}\right)^2$$
$$-0.0000001V_a - 0.18414392\left(\frac{V_{beff}}{V_a + V_{beff}}\right)\Bigg)$$
$$+\frac{2.597758994 + 0.040197991V_a + 0.596946197\left(\frac{V_{beff}}{V_a + V_{beff}}\right) + 0.00806974R_{10} - 0.000106102\left(R_{10}\right)^2 - 0.010347472R_{14}}{1 + e^{\left(-0.847277886 - 0.80288457\log\left|G_b^*\right| + 1.540388406\log\delta_b\right)}} \quad (9)$$

With $|E^*|$ = dynamic modulus (105 psi); $|G^*|$ est the dynamic shear modulus of the binder; δ_b is the phase angle of the binder; $P_{0.08}$ = percent passing 0.08 mm sieve; R_5 = cumulative percentage of the sieve 5 mm; R_{10} = the percentage of cumulative screen oversize 10 mm; R_{14} = the percentage of cumulative screen oversize 14 mm; V_a = void percentage; V_{beff} = Binder content effective in volume percentage.

Correlating the predicted modulus values with the new model shows a good correlation with an R^2 = 0.9175 and p = 0.00. Figure 6 shows the results of the correlation.

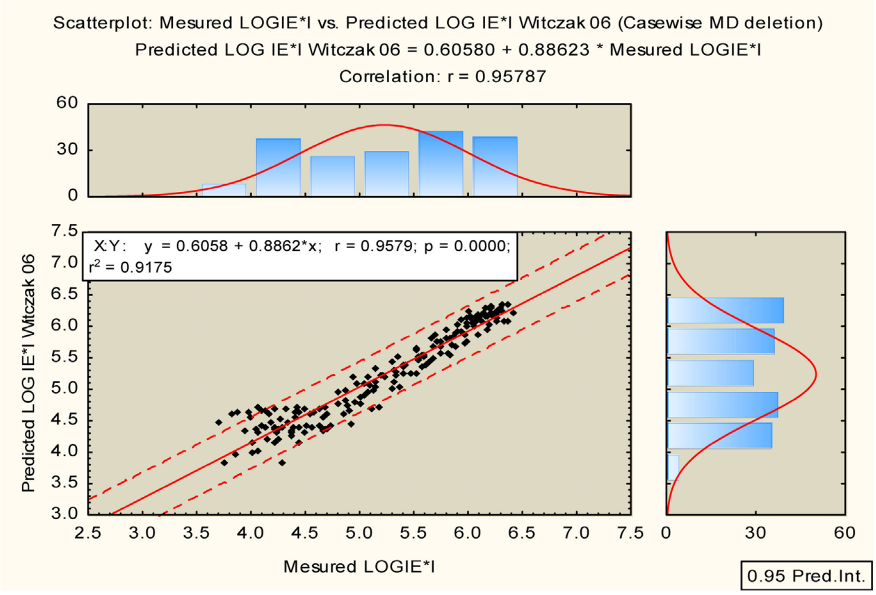

Figure 6. Correlation $p < 0.005$ log$|E^*|$ predicted, optimized and log$|E^*|$ observed.

4. Conclusion

The approach of Witczak's sigmoidal model by sieve mesh (1999 and 2006) is a simple replacement of US sieve mesh ρ_{200} (0.075 mm), ρ_4 (4.76 mm), ρ_{38} (9.5 mm) and ρ_{34} (19 mm) by AFNOR and Lc sieve mesh respectively $P_{0.08}$ (0.08 mm), R_5 (5 mm), R_{10} (10 mm) and R_{14} (14 mm).The evaluation Witczak's model 1999 shows that the sieve mesh approach does not compromise the ability of this model to predict asphalt formulated according to AFNOR and LC methods. The evaluation of the Witczak 2006 model presents a less accurate than the 1999 model. But accuracy remains statistically valid to predict the dynamic modulus of asphalt mixtures. Solver MS-Excel is a great tool adjustment through its non-linear GRG module. The adjustment of the model approached Witczak 1999 is more accurate than the adjustment of the approximate 2006 model. Dynamic modulus of HMA designed with basalt of Diack and quartzite Diack Bakel is well predicted by Witczak's of 1999 and 2006 model by approached mesh sieve. For best accuracy, however, the optimized models are recommended. In perspective it will be important for a better reliability of the prediction to calibrate these new models with a larger database including different types of HMA.

Acknowledgements

The authors would like to acknowledge the research group of the "Ecole de Technologies Supérieure" of Montréal.

Conflicts of Interest

The authors declare no conflicts of interest regarding the publication of this paper.

References

[1] Hammons, M., Teem, D. and Green, J. (2007) Instrumentation Data Interpretation. State Materials Office, State of Florida.

[2] Li, N., *et al.* (2020) A Prediction Model of Permanent Strain of Unbound Gravel Materials Based on Performance of Single-Size Gravels under Repeated Loads. *Construction and Building Materials*, **246**, Article ID: 118492. https://doi.org/10.1016/j.conbuildmat.2020.118492

[3] Georgouli, K., Loizos, A. and Plati, C. (2015) Calibration of Dynamic Modulus Predictive Model. *Construction and Building Materials*, **102**, 65-75. https://doi.org/10.1016/j.conbuildmat.2015.10.163

[4] Khattab, A.M., El-Badawy, S.M., Al Hazmi, A.A. and Elmwafi, M. (2014) Evaluation of Witczak E* Predictive Models for the Implementation of AASHTO-Ware-Pavement ME Design in the Kingdom of Saudi Arabia. *Construction and Building Materials*, **64**, 360-369. https://doi.org/10.1016/j.conbuildmat.2014.04.066

[5] AAT (Advanced Asphalt Technologies) (2011) A Manual for Design of Hot Mix Asphalt with Commentary (NCHRP Report 673). National Research Council, Transportation Research Board, Washington DC.

[6] Andrei, D., Mirza, W. and Witczak, W. (1999) Development of a Revised Predictive

Model for the Dynamic (Complex) Modulus of Asphalt Mixtures. NCHRP Report 1-37A.

[7] You, Z. and Buttlar, W. (2004) Discrete Element Modeling to Predict the Modulus of Asphalt Concrete Mixtures. *Journal of Materials in Civil Engineering*, **16**, 140-146. https://doi.org/10.1061/(ASCE)0899-1561(2004)16:2(140)

[8] You, Z. and Buttlar, W. (2005) Application of Discrete Element Modeling Techniques to Predict the Complex Modulus of Asphalt-Aggregate Hollow Cylinders Subjected to Internal Pressure. *Transportation Research Record Journal of the Transportation Research Board*, **1929**, 218-226. https://doi.org/10.3141/1929-26

[9] You, Z. and Goh, S.W. (2012) Predictive Models for Dynamic Modulus Using Weighted Least Square Nonlinear Multiple Regression Model. *Canadian Journal of Civil Engineering*, **39**, 589-597. https://doi.org/10.1139/l2012-035

[10] Bari, J. and Witczak, M.W. (2006) Development of a New Revised Version of the Witczak E* Predictive Model for Hot Mix Asphalt Mixtures. *Journal of the Association of Asphalt Paving Technologists*, **75**, 381-424.

[11] Christensen, D.W., *et al*. (2003) Hirsch Model for Estimating the Modulus of Asphalt Concrete. *Journal of Association of Asphalt Paving Technologists*, **72**, 97-121.

[12] NFEN 13108-1 (2007) Hot Mixtures Asphalt, Material Specifications Part 1: HMA. French Standards Association (AFNOR).

[13] LC 26-700 (2009) Determination of the Complex Modulus of HMA. Ministry of Transportation Laboratory, Quebec.

[14] Touhara, R. (2012) Etude de la résistance en fatigue des matériaux bitumineux, Mémoire de Maitrise, Ecole de Technologie Supérieure, Montréal Qc.

Appendix: Data for Statistical Analysis

Mixtures	Temperatures and frequencies		Volumetric composition of mixtures							Test on bitumen 35/50 ou PG 70-16				Dynamic modulus test laboratory test results		Witczak's 1999 model (MEPDG)	Witczak 2006 model (MEPDG)
	T °C	f. Hz	ρ34- 19.00 - 14 mm	ρ38- 9.500 - 10 mm	ρ4- 4.7600 - 5 mm	ρ200- 0.075 - 0.08 mm	V_{beff}	Va	A	Viscosity η (10^6 Pa.s)	VTS	δb (°)	IG*I Module Dynamic Modulus (DSR test) (psi)	IE*I (psi)	δ (°)	IE*I (psi)	IE*I (psi)
BDF	−0.11484506	10.0472826	1	8	28	8	11.34	8.77	14.2392	2.08163462	−4.9303	3.64441901	916.182811	2,291,337.61	7.45477925	1,210,297.381	7,668,937.03
BDF	−0.17177768	3.01465895	1	8	28	8	11.34	8.77	14.2392	2.12809128	−4.9303	6.86064288	866.262618	2,063,567.16	8.33227858	911,503.2797	6,147,775.18
BDF	−0.16600072	1.00487491	1	8	28	8	11.34	8.77	14.2392	2.12332779	−4.9303	6.51793241	794.210857	1,859,340.45	9.20601144	686,683.8367	6,163,390.03
BDF	−0.13361162	0.30146788	1	8	28	8	11.34	8.77	14.2392	2.09682854	−4.9303	6.22597098	652.178106	1,631,950.11	10.4005233	492,989.5483	6,038,348.22
BDF	−0.15027567	0.10048827	1	8	28	8	11.34	8.77	14.2392	2.11041839	−4.9303	6.84430949	577.603468	1,454,126.46	11.0535909	361,762.2698	5,683,056.22
BDF	10.0207844	10.0532669	1	8	28	8	11.34	8.77	14.2392	0.06104662	−4.9303	5.0917143	814.556336	1,574,781.67	11.6630179	376,195.2083	6,758,109.04
BDF	9.94728906	3.01594813	1	8	28	8	11.34	8.77	14.2392	0.06246433	−4.9303	11.1561055	750.623093	1,346,510.71	13.0939069	266,943.4389	4,921,449.26
BDF	9.93841748	1.00452044	1	8	28	8	11.34	8.77	14.2392	0.06263782	−4.9303	14.3708818	678.714916	1,133,489.39	14.6918064	192,501.261	4,293,957.74
BDF	9.98368722	0.30144998	1	8	28	8	11.34	8.77	14.2392	0.06175788	−4.9303	19.4496154	575.887026	927,669.744	16.5705198	133,242.3532	3,552,076.94
BDF	9.9725091	0.10038991	1	8	28	8	11.34	8.77	14.2392	0.06197392	−4.9303	27.262347	495.559167	762,551.562	18.1700157	95,883.74145	2,842,367.47
BDF	19.9685955	10.0535104	1	8	28	8	11.34	8.77	14.2392	0.00368965	−4.9303	17.4031234	601.52195	913,646.296	18.4030165	131,339.9082	3,799,350.87
BDF	19.9655083	3.01204819	1	8	28	8	11.34	8.77	14.2392	0.00369255	−4.9303	25.7093848	486.139494	711,357.672	20.6203447	91,495.3866	2,918,216.43
BDF	19.9582191	1.00466551	1	8	28	8	11.34	8.77	14.2392	0.0036994	−4.9303	30.8371738	375.165254	553,920.83	22.6034087	66,193.19964	2,423,984.35
BDF	19.9278062	0.30141668	1	8	28	8	11.34	8.77	14.2392	0.00372814	−4.9303	36.4035093	263.912773	405,880.599	25.4169001	46,966.73523	1,943,056.15
BDF	19.9606592	0.10049039	1	8	28	8	11.34	8.77	14.2392	0.00369711	−4.9303	44.3154074	227.583289	294,956.589	27.9473783	34,574.52292	1,624,261.99
BDF	29.8351333	10.0598564	1	8	28	8	11.34	8.77	14.2392	0.00037844	−4.9303	35.0014984	350.953452	468,929.188	25.9965025	56,070.53311	2,198,746.19
BDF	29.8489495	3.01987169	1	8	28	8	11.34	8.77	14.2392	0.00037735	−4.9303	44.2050338	225.289547	330,752.087	28.8285446	39,890.09239	1,620,743.91
BDF	29.8387026	1.00524211	1	8	28	8	11.34	8.77	14.2392	0.00037816	−4.9303	50.2280149	126.986387	232,716.584	31.7376712	29,674.1178	1,191,791.37
BDF	29.8588742	0.30153569	1	8	28	8	11.34	8.77	14.2392	0.00037657	−4.9303	53.6978965	44.469069	151,795.713	34.2194037	21,803.47975	737,107.16
BDF	29.816896	0.10040112	1	8	28	8	11.34	8.77	14.2392	0.00037989	−4.9303	58.1311473	61.7935544	100,876.494	36.6690388	16,818.27282	799,711.56
BDF	39.5592949	10.0205943	1	8	28	8	11.34	8.77	14.2392	5.9361E−05	−4.9303	52.5313381	134.527441	202,490.281	34.5227993	29,389.83066	1,182,523.87
BDF	39.5699807	3.01664778	1	8	28	8	11.34	8.77	14.2392	5.9252E−05	−4.9303	60.7607668	53.6936408	129,050.987	36.9966681	21,642.65707	729,965.04
BDF	39.5983539	1.00401606	1	8	28	8	11.34	8.77	14.2392	5.8961E−05	−4.9303	67.3392148	23.8125803	82,779.9231	38.9739953	16,634.58617	478,380.98
BDF	39.5774447	0.30154867	1	8	28	8	11.34	8.77	14.2392	5.9175E−05	−4.9303	67.5823376	16.3906146	49,436.5059	41.0739191	12,774.83761	406,621.28
BDF	39.5739282	0.10048905	1	8	28	8	11.34	8.77	14.2392	5.9211E−05	−4.9303	68.8607733	67.1369536	31,676.902	41.7565005	10,229.97225	732,834.74
BDF	54.0749205	10.0539698	1	8	28	8	11.34	8.77	14.2392	6.5562E−06	−4.9303	68.2407958	14.5601578	46,675.4254	43.7014272	14,968.101	383,874.96
BDF	54.0638944	3.01204819	1	8	28	8	11.34	8.77	14.2392	6.5658E−06	−4.9303	70.464758	4.87522601	27,958.8655	43.3037334	11,583.59064	237,769.44
BDF	54.0698369	1.00654507	1	8	28	8	11.34	8.77	14.2392	6.5607E−06	−4.9303	78.2094929	9.56044226	17,558.5413	42.1049774	9354.020612	291,313.65
BDF	54.0932081	0.30143836	1	8	28	8	11.34	8.77	14.2392	6.5404E−06	−4.9303	75.5092721	19.6687803	11,009.1005	40.1422943	7552.722807	405,333.50
BDF	54.0770426	0.10049242	1	8	28	8	11.34	8.77	14.2392	6.5544E−06	−4.9303	79.3911228	74.4823983	7456.42731	37.9602201	6342.891285	690,724.08
BDC	0.14847441	10.0503147	3	17	50	4	11	8.91	14.2392	1.88028298	−4.9303	3.49393748	915.646643	2,045,179.08	7.71949902	923,709.1634	9,825,318.98
BDC	0.21004821	3.01568813	3	17	50	4	11	8.91	14.2392	1.83623549	−4.9303	6.75944172	867.017156	1,825,803.45	9.12726814	684,308.6439	7,787,845.95

Continued

BDC	0.22865472	1.00468869	3	17	50	4	11	8.91	14.2392	1.8231406	−4.9303	6.59166808	797.644449	1,616,159.99	10.5100648	513,338.5739	7,737,295.00
BDC	0.11403329	0.30146816	3	17	50	4	11	8.91	14.2392	1.90540632	−4.9303	6.47211826	657.261173	1,390,057.49	12.6732943	375,117.3644	7,502,155.78
BDC	0.16946427	0.10049241	3	17	50	4	11	8.91	14.2392	1.86514357	−4.9303	7.53750712	582.523183	1,169,179.64	15.2937661	272,232.9953	6,885,564.56
BDC	9.78889979	10.0390843	3	17	50	4	11	8.91	14.2392	0.06564045	−4.9303	4.91237237	818.469453	1,431,374.72	12.5607237	303,883.5695	8,641,122.01
BDC	9.79486882	3.0090286	3	17	50	4	11	8.91	14.2392	0.06551769	−4.9303	10.9983893	753.953225	1,198,326.53	14.9458392	213,818.9229	6,217,730.04
BDC	9.80409112	1.00563219	3	17	50	4	11	8.91	14.2392	0.06532849	−4.9303	14.1966027	682.21095	974,972.666	18.0977192	154,104.5678	5,410,199.77
BDC	9.84189095	0.30145	3	17	50	4	11	8.91	14.2392	0.06455908	−4.9303	19.2276692	579.696301	746,183.538	22.1841617	106,765.6642	4,462,963.10
BDC	9.7986725	0.10040866	3	17	50	4	11	8.91	14.2392	0.06543958	−4.9303	26.9383462	499.730369	563,614.751	26.3104645	77,139.11068	3,562,050.60
BDC	20.3069283	10.0307091	3	17	50	4	11	8.91	14.2392	0.00338642	−4.9303	17.9475929	593.17194	770,765.346	22.2695279	100,098.7775	4,651,964.37
BDC	20.3149364	3.01204819	3	17	50	4	11	8.91	14.2392	0.00337958	−4.9303	26.3277482	476.233469	561,682.715	26.9193824	69,753.40627	3,553,905.58
BDC	20.3032369	1.00401606	3	17	50	4	11	8.91	14.2392	0.00338958	−4.9303	31.4922101	364.698454	394,639.958	31.6006444	50,525.1017	2,934,873.92
BDC	20.1520879	0.30151622	3	17	50	4	11	8.91	14.2392	0.00352172	−4.9303	36.8033643	257.148228	254,642.036	36.6166016	36,301.44258	2,356,369.16
BDC	20.0650168	0.10049241	3	17	50	4	11	8.91	14.2392	0.00360035	−4.9303	44.4773605	225.005717	162,722.946	40.4786334	27,029.51798	1,982,201.78
BDC	30.1979938	10.020902	3	17	50	4	11	8.91	14.2392	0.0003509	−4.9303	35.6835974	341.908295	351,143.561	34.2606021	42,970.9345	2,660,345.60
BDC	30.158609	3.01034967	3	17	50	4	11	8.91	14.2392	0.00035378	−4.9303	44.7871336	218.224544	219,672.376	38.8499103	30,739.66175	1,950,160.86
BDC	30.2015492	1.00806452	3	17	50	4	11	8.91	14.2392	0.00035064	−4.9303	50.931944	120.481397	136,349.56	41.8356226	22,850.85775	1,411,135.37
BDC	30.2004703	0.30146215	3	17	50	4	11	8.91	14.2392	0.00035072	−4.9303	54.2566499	40.4181942	79,760.5141	42.4319329	16,830.86172	849,828.59
BDC	30.198284	0.10038392	3	17	50	4	11	8.91	14.2392	0.00035088	−4.9303	58.6056193	59.0172814	48,993.242	40.9098628	12,973.57781	945,104.28
BDC	40.4573195	10.0891469	3	17	50	4	11	8.91	14.2392	5.0873E−05	−4.9303	53.9836022	118.458554	121,083.63	44.0927827	22,078.19975	1,344,961.98
BDC	40.5204679	3.02121729	3	17	50	4	11	8.91	14.2392	5.0329E−05	−4.9303	62.0839614	43.0107125	70,191.5343	43.5470032	16,248.10298	790,005.86
BDC	40.5161152	1.00401606	3	17	50	4	11	8.91	14.2392	5.0367E−05	−4.9303	68.6625614	20.9589774	43,844.1825	40.2142615	12,549.44311	535,556.71
BDC	40.4982977	0.30146215	3	17	50	4	11	8.91	14.2392	5.052E−05	−4.9303	68.6210342	20.9147106	28,102.9495	34.7538524	9673.594195	535,304.54
BDC	40.5051726	0.10049949	3	17	50	4	11	8.91	14.2392	5.046E−05	−4.9303	69.731563	73.589921	20,620.8874	29.4538585	7772.176219	914,371.64
BDC	55.3654519	10.0877193	3	17	50	4	11	8.91	14.2392	5.5374E−06	−4.9303	68.56248	22.0357368	32,392.4092	37.7332386	11,282.34065	547,990.63
BDC	55.3539165	3.01738063	3	17	50	4	11	8.91	14.2392	5.5456E−06	−4.9303	69.9400416	10.2297404	23,478.4085	29.1051442	8765.213903	387,210.21
BDC	55.4172026	1.00937588	3	17	50	4	11	8.91	14.2392	5.5004E−06	−4.9303	77.8494551	0.37554088	19,332.5449	22.4188032	7094.582416	104,246.70
BDC	55.3401578	0.30150769	3	17	50	4	11	8.91	14.2392	5.5555E−06	−4.9303	75.1739137	6.89990411	16,476.8457	17.6326354	5766.110804	310,914.57
BDC	54.4	0.1	3	17	50	4	11	8.91	14.2392	6.2808E−06	−4.9303	79.551876	68.0027194	14,935	14.7	4967.126873	801,751.44
GDF	0.91366976	10.0493043	2	10	26	10	11.64	5.28	14.2392	1.40364346	−4.9303	3.12003647	913.363935	1,945,855.5	8.32604637	1,728,227.122	15,815,706.76
GDF	0.9604202	3.01481783	2	10	26	10	11.64	5.28	14.2392	1.37901074	−4.9303	6.62835593	867.050268	1,669,844.61	9.29360797	1,272,353.469	12,279,368.28
GDF	0.93101915	1.00493928	2	10	26	10	11.64	5.28	14.2392	1.39444825	−4.9303	6.7759871	801.679463	1,485,114.91	11.0193887	954,192.7483	12,003,460.14
GDF	0.93807777	0.30147519	2	10	26	10	11.64	5.28	14.2392	1.39072541	−4.9303	7.32398628	670.851515	1,270,227.34	13.201413	681,530.8249	11,254,539.54
GDF	0.94223131	0.10049233	2	10	26	10	11.64	5.28	14.2392	1.38853968	−4.9303	9.19986803	591.698044	1,077,091.84	15.5804412	495,486.2977	9,989,999.96
GDF	12.7895703	10.0431208	2	10	26	10	11.64	5.28	14.2392	0.02636181	−4.9303	7.66565294	763.39781	1,108,988.73	16.3915186	440,749.2547	11,348,915.60
GDF	12.7479521	3.01508147	2	10	26	10	11.64	5.28	14.2392	0.02668719	−4.9303	14.4536316	684.148111	876,714.196	19.3984558	308,876.2275	8,473,684.44
GDF	12.753971	1.00502513	2	10	26	10	11.64	5.28	14.2392	0.02663987	−4.9303	18.3606831	599.30268	677,466.802	22.5528796	221,394.9542	7,303,360.58
GDF	12.7208499	0.3014621	2	10	26	10	11.64	5.28	14.2392	0.02690139	−4.9303	23.8771513	495.310836	486,410.468	27.1133126	154,482.0938	6,039,873.02

Continued

GDF	12.7771036	0.10040868	2	10	26	10	11.64	5.28	14.2392	0.02645883	−4.9303	32.3609763	422.683701	341,894.876	31.4825821	110,659.354	4,850,267.29
GDF	22.1228003	10.0393271	2	10	26	10	11.64	5.28	14.2392	0.00215842	−4.9303	20.9685642	547.693688	564,580.228	26.2727187	170,246.3942	6,660,090.94
GDF	22.1313662	3.01813314	2	10	26	10	11.64	5.28	14.2392	0.00215392	−4.9303	29.6145232	425.037238	387,217.28	30.793245	118,742.884	5,112,828.35
GDF	22.1411563	1.00477362	2	10	26	10	11.64	5.28	14.2392	0.00214879	−4.9303	35.0363219	310.506437	257,364.896	35.315075	86,019.94632	4,169,996.98
GDF	22.1161199	0.30154219	2	10	26	10	11.64	5.28	14.2392	0.00216193	−4.9303	40.3065339	200.675767	155,728.296	39.2201889	61,374.43035	3,264,781.55
GDF	22.1598994	0.10049241	2	10	26	10	11.64	5.28	14.2392	0.00213901	−4.9303	47.6574683	176.303525	95,513.9453	41.495881	45,478.72847	2,785,004.04
GDF	32.5854758	10.0540723	2	10	26	10	11.64	5.28	14.2392	0.00021624	−4.9303	40.1586964	283.708234	211,805.518	38.8314608	72,616.50844	3,713,730.78
GDF	32.6482355	3.01813314	2	10	26	10	11.64	5.28	14.2392	0.00021357	−4.9303	49.3845244	164.909778	122,813.913	41.8576285	51,878.13052	2,649,983.96
GDF	32.6268499	1.00446499	2	10	26	10	11.64	5.28	14.2392	0.00021448	−4.9303	55.5451048	82.4570629	74,824.2659	42.6619687	38,948.93662	1,849,469.02
GDF	32.6366237	0.30149673	2	10	26	10	11.64	5.28	14.2392	0.00021406	−4.9303	58.1202504	18.6672783	42,479.5676	41.4253257	28,954.75292	954,758.69
GDF	32.6139912	0.10049241	2	10	26	10	11.64	5.28	14.2392	0.00021502	−4.9303	61.5068619	47.8309001	27,132.6836	38.2839747	22,550.93461	1,368,580.26
GDF	43.121377	10.0733295	2	10	26	10	11.64	5.28	14.2392	3.2677E−05	−4.9303	58.0126297	76.2281762	63,524.8626	45.4567504	38,279.00358	1,735,928.15
GDF	43.1134247	3.01204819	2	10	26	10	11.64	5.28	14.2392	3.2719E−05	−4.9303	65.3040681	19.6163769	36,780.7312	42.3334864	28,492.43059	895,663.56
GDF	43.1553698	1.00654635	2	10	26	10	11.64	5.28	14.2392	3.2497E−05	−4.9303	72.0819351	17.3302903	23,168.9483	37.6760989	22,159.70932	790,597.87
GDF	43.1365971	0.30152269	2	10	26	10	11.64	5.28	14.2392	3.2596E−05	−4.9303	71.2567835	36.5200794	15,307.1721	30.6543858	17,228.26284	1,096,150.66
GDF	43.1298645	0.10048821	2	10	26	10	11.64	5.28	14.2392	3.2632E−05	−4.9303	72.042133	93.0674473	11,546.217	23.8342199	13,965.92599	1,616,378.31
GDF	57.4814459	10.0850738	2	10	26	10	11.64	5.28	14.2392	4.2332E−06	−4.9303	68.5937861	42.2830066	18,253.9544	34.0607718	20,913.57979	1,199,767.99
GDF	57.4512264	3.01204819	2	10	26	10	11.64	5.28	14.2392	4.2491E−06	−4.9303	68.4755021	20.8944389	13,431.3645	24.7918545	16,335.49865	888,838.08
GDF	57.4638816	1.00401606	2	10	26	10	11.64	5.28	14.2392	4.2424E−06	−4.9303	76.7436615	24.1979981	10,945.9373	17.9009051	13,296.42688	870,809.13
GDF	57.4649567	0.3014708	2	10	26	10	11.64	5.28	14.2392	4.2419E−06	−4.9303	74.1551329	72.8536287	9656.81436	13.0450172	10,847.88723	1,428,370.58
GDF	57.4871958	0.10048821	2	10	26	10	11.64	5.28	14.2392	4.2301E−06	−4.9303	80.9264103	23.7750694	8707.77945	9.64657789	9175.653212	831,475.77
GDD	0.09261823	10.040201	5	21	37	9	11.5	2.19	14.2392	1.9212063	−4.9303	3.52491616	915.771162	2,612,507.65	6.685383	2,765,098.761	32,920,624.02
GDD	0.14033187	3.01386816	5	21	37	9	11.5	2.19	14.2392	1.88619087	−4.9303	6.77616546	866.917216	2,348,150.09	7.73769046	2,044,917.579	26,131,567.79
GDD	0.14912447	1.00502513	5	21	37	9	11.5	2.19	14.2392	1.87981217	−4.9303	6.57506445	797.021499	2,127,750.13	10.2600661	1,531,215.788	26,003,852.40
GDD	0.21741496	0.30144998	5	21	37	9	11.5	2.19	14.2392	1.83103907	−4.9303	6.57623855	659.243664	1,828,861.76	12.4560758	1,086,971.758	25,045,531.43
GDD	0.19023634	0.10049847	5	21	37	9	11.5	2.19	14.2392	1.85028796	−4.9303	7.58243214	582.819516	1,546,907.62	14.8999694	794,403.5778	23,055,921.96
GDD	9.99615879	10.0394831	5	21	37	9	11.5	2.19	14.2392	0.06151778	−4.9303	5.07239006	814.974798	1,861,530.22	12.4698703	869,757.293	28,680,516.56
GDD	9.9931124	3.01935013	5	21	37	9	11.5	2.19	14.2392	0.06157634	−4.9303	11.2039849	749.615398	1,512,858.41	15.7620458	609,942.6473	20,679,108.96
GDD	10.001568	1.00401606	5	21	37	9	11.5	2.19	14.2392	0.06141396	−4.9303	14.4533518	677.060405	1,238,345.39	19.5843992	436,899.2	17,971,086.43
GDD	9.98754464	0.30146212	5	21	37	9	11.5	2.19	14.2392	0.06168351	−4.9303	19.4556643	575.782786	926,632.49	24.7817297	303,217.3389	14,853,415.54
GDD	9.98689178	0.10040617	5	21	37	9	11.5	2.19	14.2392	0.06169609	−4.9303	27.2891121	495.211772	670,252.844	30.4854157	217,043.2266	11,824,486.09
GDD	20.1269103	10.0413834	5	21	37	9	11.5	2.19	14.2392	0.00354426	−4.9303	17.6571245	597.620284	958,620.144	24.4468849	294,269.9657	15,769,323.09
GDD	20.0560246	3.0135854	5	21	37	9	11.5	2.19	14.2392	0.00360858	−4.9303	25.8690868	483.572582	665,922.301	30.4486721	205,556.777	12,093,283.03
GDD	20.1064456	1.00401606	5	21	37	9	11.5	2.19	14.2392	0.0035627	−4.9303	31.1181391	370.65869	437,246.323	37.7468459	147,282.0775	9,961,122.23
GDD	20.0685226	0.30147077	5	21	37	9	11.5	2.19	14.2392	0.00359715	−4.9303	36.654363	259.66188	248,631.576	45.4172653	104,202.5862	7,939,936.36
GDD	20.0976543	0.10049645	5	21	37	9	11.5	2.19	14.2392	0.00357066	−4.9303	44.527942	224.202282	137,255.907	51.5662283	76,481.06838	6,621,760.55
GDD	30.0799395	10.0562082	5	21	37	9	11.5	2.19	14.2392	0.00035961	−4.9303	35.4616724	344.846181	371,640.071	41.35833	123,927.6984	8,975,302.46

Continued

GDD	30.0560471	3.02306788	5	21	37	9	11.5	2.19	14.2392	0.0003614	−4.9303	44.5945339	220.554419	204,470.748	48.4594628	88,137.71521	6,573,690.91
GDD	30.0144695	1.00401606	5	21	37	9	11.5	2.19	14.2392	0.00036454	−4.9303	50.5693758	123.808965	108,713.428	54.2458142	65,473.36049	4,795,309.25
GDD	30.0015039	0.30148487	5	21	37	9	11.5	2.19	14.2392	0.00036553	−4.9303	53.9316614	42.7473578	50,611.4689	58.3600607	48,077.73687	2,918,352.87
GDD	30.0455527	0.10049646	5	21	37	9	11.5	2.19	14.2392	0.00036219	−4.9303	58.4161492	60.0953107	25,125.303	60.3199869	36,803.41605	3,187,840.58
GDD	40.1621228	10.0510663	5	21	37	9	11.5	2.19	14.2392	5.3505E−05	−4.9303	53.5109793	123.645124	100,024.045	56.4833308	63,472.97614	4,605,498.16
GDD	40.1058896	3.02540539	5	21	37	9	11.5	2.19	14.2392	5.4023E−05	−4.9303	61.5155706	47.5308852	47,101.7243	58.4891146	46,829.21905	2,772,149.95
GDD	40.0614253	1.00401606	5	21	37	9	11.5	2.19	14.2392	5.4437E−05	−4.9303	68.0150073	22.2557755	23,405.1575	57.488496	36,050.52238	1,845,058.59
GDD	40.1875911	0.30148377	5	21	37	9	11.5	2.19	14.2392	5.3272E−05	−4.9303	68.2770982	19.3103215	11,528.4893	53.1389633	27,460.01294	1,728,817.20
GDD	40.1462034	0.1005042	5	21	37	9	11.5	2.19	14.2392	5.3651E−05	−4.9303	69.3990611	71.0473782	6694.44604	45.945857	22,016.46557	3,018,417.88
GDD	55.0037626	10	5	21	37	9	11.5	2.19	14.2392	5.8035E−06	−4.9303	68.4946979	19.5783849	17,445.6221	51.3889644	31,999.40215	1,735,157.72
GDD	55.0480684	2.99864315	5	21	37	9	11.5	2.19	14.2392	5.7701E−06	−4.9303	70.0896294	8.86637576	10,189.4389	39.4010067	24,718.883	1,209,802.35
GDD	55.0171667	1.00215363	5	21	37	9	11.5	2.19	14.2392	5.7934E−06	−4.9303	77.9860066	2.99792658	7150.0433	28.6441023	19,989.16559	716,723.87
GDD	55.0166963	0.30165913	5	21	37	9	11.5	2.19	14.2392	5.7937E−06	−4.9303	75.2791189	0.78140181	5668.73067	20.4529994	16,170.53133	445,922.34
GDD	55.0121392	0.10048232	5	21	37	9	11.5	2.19	14.2392	5.7971E−06	−4.9303	79.8477553	54.2324205	4996.475	15.8370262	13,578.99085	2,418,652.76
GDC	0.413688	10.0587111	3	16	37	8	11.12	6.95	14.2392	1.69815982	−4.9303	3.35372725	914.976698	1602553.7	8.64477279	1,405,669.017	13,368,068.27
GDC	0.42833745	3.01932807	3	16	37	8	11.12	6.95	14.2392	1.68865936	−4.9303	6.71210876	867.222265	1,397,263.01	9.92835248	1,043,198.016	10,513,479.33
GDC	0.45047181	1.00519364	3	16	37	8	11.12	6.95	14.2392	1.67441118	−4.9303	6.64259299	799.201025	1,225,791.23	11.8725263	779,480.3148	10,391,697.82
GDC	0.47184475	0.3014621	3	16	37	8	11.12	6.95	14.2392	1.66077363	−4.9303	6.83587437	663.77895	1,033,222.59	14.1127244	557,127.1099	9,910,715.28
GDC	0.41513403	0.10049241	3	16	37	8	11.12	6.95	14.2392	1.69721953	−4.9303	8.06798113	585.849181	848,340.297	16.6902439	409,276.4073	9,032,776.65
GDC	10.2855913	10.050509	3	16	37	8	11.12	6.95	14.2392	0.05621661	−4.9303	5.30366245	810.013418	1,017,564.41	15.1125289	447,466.1747	11,300,310.27
GDC	10.3033375	3.01204819	3	16	37	8	11.12	6.95	14.2392	0.05590785	−4.9303	11.5337137	742.715543	803,981.642	17.9845141	313,203.2882	8,186,666.98
GDC	10.2816355	1.00536283	3	16	37	8	11.12	6.95	14.2392	0.05628568	−4.9303	14.8231948	669.640912	633,980.995	21.5664117	225,817.9819	7,124,501.31
GDC	10.2379991	0.30150323	3	16	37	8	11.12	6.95	14.2392	0.05705368	−4.9303	19.8496569	568.947217	464,749.038	25.6830699	157,607.3032	5,904,914.80
GDC	10.282075	0.1004087	3	16	37	8	11.12	6.95	14.2392	0.05627801	−4.9303	27.8370188	488.007791	337,945.369	30.6879667	112,515.6297	4,700,941.73
GDC	20.1638394	10.0598564	3	16	37	8	11.12	6.95	14.2392	0.00351125	−4.9303	17.7165694	596.708759	490,626.28	26.2231505	157,138.7837	6,338,480.22
GDC	20.1627364	3.01987169	3	16	37	8	11.12	6.95	14.2392	0.00351223	−4.9303	26.0577972	480.547083	338,818.216	30.9680776	109,322.8881	4,854,077.80
GDC	20.1713519	1.00603622	3	16	37	8	11.12	6.95	14.2392	0.00350457	−4.9303	31.2413855	368.689935	228,511.732	35.4375962	78,838.66523	4,013,340.19
GDC	20.1535057	0.3014394	3	16	37	8	11.12	6.95	14.2392	0.00352045	−4.9303	36.8058926	257.105649	141,024.718	39.2608292	55,791.05881	3,199,675.59
GDC	20.2950439	0.10048736	3	16	37	8	11.12	6.95	14.2392	0.00339661	−4.9303	44.8331561	219.370963	86,634.3288	41.2130594	40,656.22834	2,655,505.58
GDC	29.9243066	10.0738014	3	16	37	8	11.12	6.95	14.2392	0.00037146	−4.9303	35.1691143	348.726506	201,236.85	37.7335585	67,612.36305	3,667,285.26
GDC	29.9690609	3.01204819	3	16	37	8	11.12	6.95	14.2392	0.00036801	−4.9303	44.4310288	222.538337	121,528.931	41.4607717	47,865.96239	2,685,888.54
GDC	29.960934	1.00452339	3	16	37	8	11.12	6.95	14.2392	0.00036863	−4.9303	50.4654753	124.771518	74,085.4511	42.747014	35,579.81012	1,963,138.68
GDC	29.9595055	0.30146215	3	16	37	8	11.12	6.95	14.2392	0.00036874	−4.9303	53.862896	43.2498118	42,563.2884	42.1394833	26,154.10862	1,202,611.98
GDC	29.9449639	0.10041287	3	16	37	8	11.12	6.95	14.2392	0.00036986	−4.9303	58.2909719	60.8299171	26,972.2542	39.9091768	20,123.09243	1,313,333.01
GDC	40.2156972	10.0225803	3	16	37	8	11.12	6.95	14.2392	5.3016E−05	−4.9303	53.5971084	122.696772	63,518.6652	44.2004393	34,238.33166	1,869,514.96
GDC	40.1984039	3.01572142	3	16	37	8	11.12	6.95	14.2392	5.3173E−05	−4.9303	61.6436012	46.5034933	37,408.5496	41.4933069	25,266.29303	1,123,652.55
GDC	40.2513695	1.00755846	3	16	37	8	11.12	6.95	14.2392	5.2694E−05	−4.9303	68.287478	21.6867725	24,224.4194	36.4036963	19,430.40415	748,548.06

Continued

GDC	40.2258792	0.30140161	3	16	37	8	11.12	6.95	14.2392	5.2924E−05	−4.9303	68.3198447	19.5040208	16,223.6791	29.5586024	14,930.06875	714,655.49
GDC	40.2156875	0.10048838	3	16	37	8	11.12	6.95	14.2392	5.3016E−05	−4.9303	69.4637318	71.5346614	12,577.1199	23.5332957	11,975.61113	1,238,387.73
GDC	54.921576	10.1313891	3	16	37	8	11.12	6.95	14.2392	5.866E−06	−4.9303	68.4768383	19.0597114	17,931.6945	30.8788185	17,513.15425	706,357.48
GDC	54.9237794	2.99864315	3	16	37	8	11.12	6.95	14.2392	5.8643E−06	−4.9303	70.1458993	8.32835018	13,889.9334	22.4885993	13,529.58382	486,705.33
GDC	55.0136494	1.00502513	3	16	37	8	11.12	6.95	14.2392	5.796E−06	−4.9303	77.987095	3.02592751	11,367.6813	16.6300479	10,919.08857	298,944.86
GDC	54.9460801	0.30143197	3	16	37	8	11.12	6.95	14.2392	5.8472E−06	−4.9303	75.3003758	2.38249516	10,217.637	11.869553	8856.76205	278,988.37
GDC	54.9280078	0.10051262	3	16	37	8	11.12	6.95	14.2392	5.861E−06	−4.9303	79.8077743	56.2439923	9726.59434	10.5417338	7448.891435	1,008,363.48
BDD	1	10.04	1.75	14.7	40.25	6.5	12.25	5.05	14.2392	1.35851344	−4.9303	3.0837	913.039714	1,647,780	8.02	1,561,518.133	18,357,623.04
BDD	1.1	3.02	1.75	14.7	40.25	6.5	12.25	5.05	14.2392	1.30814785	−4.9303	6.613727	866.850598	1,426,510	9.31	1,143,403.492	14,156,832.83
BDD	1	1	1.75	14.7	40.25	6.5	12.25	5.05	14.2392	1.35851344	−4.9303	6.7977	801.937017	1,280,060	10.2	863,970.9689	13,807,263.91
BDD	1	0.3	1.75	14.7	40.25	6.5	12.25	5.05	14.2392	1.35851344	−4.9303	7.39	671.673136	1,112,150	12.15	618,175.1918	12,904,372.86
BDD	1	0.1	1.75	14.7	40.25	6.5	12.25	5.05	14.2392	1.35851344	−4.9303	9.3234	592.235048	957,580	14.39	450,091.6678	11,406,898.96
BDD	12.7	10.05	1.75	14.7	40.25	6.5	12.25	5.05	14.2392	0.02706743	−4.9303	7.5705213	765.172336	977,880	14.71	408,458.4034	13,127,329.85
BDD	12.7	3.02	1.75	14.7	40.25	6.5	12.25	5.05	14.2392	0.02706743	−4.9303	14.391179	685.35977	793,150	17.38	285,434.7623	9,726,690.51
BDD	12.6	1.01	1.75	14.7	40.25	6.5	12.25	5.05	14.2392	0.02787916	−4.9303	18.1269096	603.892422	631,040	20.26	207,520.4688	8,413,874.84
BDD	12.6	0.3	1.75	14.7	40.25	6.5	12.25	5.05	14.2392	0.02787916	−4.9303	23.6764464	499.090849	471,830	24.09	144,020.4241	6,925,441.55
BDD	12.7	0.1	1.75	14.7	40.25	6.5	12.25	5.05	14.2392	0.02706743	−4.9303	32.224044	424.790702	344,955	27.76	102,801.2028	5,526,240.46
BDD	22.2	10.05	1.75	14.7	40.25	6.5	12.25	5.05	14.2392	0.00211825	−4.9303	21.1003928	545.739457	518,955	23.7	155,699.8437	7,563,353.46
BDD	22.3	3.01	1.75	14.7	40.25	6.5	12.25	5.05	14.2392	0.00206741	−4.9303	29.925035	420.324203	372,505	27.86	107,744.7488	5,750,252.45
BDD	22.3	1.01	1.75	14.7	40.25	6.5	12.25	5.05	14.2392	0.00206741	−4.9303	35.3462817	305.965075	262,595	31.29	78,427.28837	4,669,952.36
BDD	22.3	0.3	1.75	14.7	40.25	6.5	12.25	5.05	14.2392	0.00206741	−4.9303	40.6341028	195.672109	169,070	34.96	55,781.59107	3,626,241.97
BDD	22.3	0.1	1.75	14.7	40.25	6.5	12.25	5.05	14.2392	0.00206741	−4.9303	47.865324	173.27208	109,330	37.68	41,563.70687	3,101,203.24
BDD	32.8	10.05	1.75	14.7	40.25	6.5	12.25	5.05	14.2392	0.00020726	−4.9303	40.5582192	278.610638	219,095	34.4	66,072.41342	4,141,648.50
BDD	32.8	3.02	1.75	14.7	40.25	6.5	12.25	5.05	14.2392	0.00020726	−4.9303	49.65884	161.870566	137,750	37.23	47,509.46454	2,944,321.12
BDD	32.7	1.01	1.75	14.7	40.25	6.5	12.25	5.05	14.2392	0.0002114	−4.9303	55.6812873	81.4580069	89,465	38.38	35,948.70652	2,051,674.99
BDD	32.7	0.3	1.75	14.7	40.25	6.5	12.25	5.05	14.2392	0.0002114	−4.9303	58.2176532	18.2651164	54,665	38.1	26,709.73795	1,043,830.00
BDD	32.8	0.1	1.75	14.7	40.25	6.5	12.25	5.05	14.2392	0.00020726	−4.9303	61.722804	47.4131853	35,670	36.46	20,690.87586	1,511,567.66
BDD	43.2	10.03	1.75	14.7	40.25	6.5	12.25	5.05	14.2392	3.2264E−05	−4.9303	58.1244848	75.1150491	76,705	40.24	35,265.31143	1,922,321.42
BDD	43.2	3.01	1.75	14.7	40.25	6.5	12.25	5.05	14.2392	3.2264E−05	−4.9303	65.400904	18.9792433	47,270	38.45	26,300.38674	973,582.84
BDD	43.2	1	1.75	14.7	40.25	6.5	12.25	5.05	14.2392	3.2264E−05	−4.9303	72.1344408	17.3170535	31,610	34.47	20,492.93985	870,204.45
BDD	43.2	0.3	1.75	14.7	40.25	6.5	12.25	5.05	14.2392	3.2264E−05	−4.9303	71.3135472	36.9143105	21,750	29.87	15,944.8262	1,218,948.48
BDD	43.2	0.1	1.75	14.7	40.25	6.5	12.25	5.05	14.2392	3.2264E−05	−4.9303	72.100964	93.5823287	16,675	25.43	12,937.05617	1,804,621.20
BDD	57.8	10.06	1.75	14.7	40.25	6.5	12.25	5.05	14.2392	4.069E−06	−4.9303	68.5425192	46.2261298	25,375	31.81	19,194.89525	1,383,842.61
BDD	57.8	3.01	1.75	14.7	40.25	6.5	12.25	5.05	14.2392	4.069E−06	−4.9303	68.15534	22.8532315	19,430	24.41	15,013.47004	1,023,530.14
BDD	57.8	1	1.75	14.7	40.25	6.5	12.25	5.05	14.2392	4.069E−06	−4.9303	76.4949352	29.2917623	16,240	19.52	12,238.66537	1,046,456.91
BDD	57.8	0.3	1.75	14.7	40.25	6.5	12.25	5.05	14.2392	4.069E−06	−4.9303	73.9411968	85.9452506	13,485	15.17	10,001.86048	1,708,749.65
BDD	57.8	0.1	1.75	14.7	40.25	6.5	12.25	5.05	14.2392	4.069E−06	−4.9303	81.049304	36.4719264	12,615	12.53	8477.437697	1,102,701.27